RSC Advances

PAPER

View Article Online
View Journal | View Issue

Cite this: *RSC Adv.*, 2018, **8**, 26517

Constraining the conformation of peptides with Au nanorods to construct multifunctional therapeutic agents with targeting, imaging, and photothermal abilities†

Linlin Xie,[a] Xiaomin Zhi,[a] Nao Xiao,[a] Chen-Jie Fang *[a] and Chun-Hua Yan [b]

Received 23rd May 2018
Accepted 10th July 2018

DOI: 10.1039/c8ra04379e

rsc.li/rsc-advances

We demonstrated an easy-to-use strategy, instead of the tedious cyclization of the peptide backbone, to constrain the freedom of an RGD (arginine, glycine, aspartic acid) sequence with gold nanorods. We further constructed a multifunctional therapeutic agent which showed targeting, application in two-photon photoluminescence imaging, and near-infrared photothermal ability, suggesting the potential of this novel strategy in the development of RGD-containing drugs for biomedical applications.

In drug discovery and development, it has been revealed that the conformation of peptides and peptidomimetics plays a predominant role in determining their biological properties and effects. Nonetheless, the conformational flexibility of peptides is a conspicuous drawback, as it leaves peptides vulnerable to proteolytic degradation and other formidable obstacles and severe limitations for bioavailability.[1–5] Considering the critical role of conformation in molecular recognition, practical methodology has long been pursued to improve the bioactivity of natural peptides using conformational constraints, *e.g.* cyclizing the molecular backbone to stabilize biologically active conformations, constraining preferred conformations with natural/unnatural amino acids as rational substitutions, and introducing *N*-methyl groups to enhance the population of a single conformation that is essential for bioactivity.[6–10] These scanning methodologies make conformational control of peptides possible, but on the other hand, it is difficult to predict or rationalize the bioactivity/effect of even simple series/analogues, due to the non-additive and cooperative effects of cyclization, substitution and *N*-methylation. Recently some novel solutions have been developed. For example, redox-switchable surfaces have been used to control the structures of peptides through electrochemistry.[11,12] A bifunctional chelating agent (BFCA) approach has also been established to constrain the conformation of peptides and mediate bioactivity,[13] while simultaneously introducing additional functions such as imaging, *etc.*[14–17] The difficulties of this strategy lie in that it has to be delicately designed with selected chelators and metal complexes for the purpose of matching the desired conformation to be constrained, as well as further providing additional functions such as photoluminescence/radioactivity that are beneficial for biomedical and therapeutic applications. However, conventional imaging techniques are unable to fulfil the urgent demands in early diagnosis, accurate staging, and image-guided cancer treatment, due to their low sensitivity and specificity, poor spatial resolution, low penetration, and/or use of harmful ionizing radiation.[18]

Here, we presented an easy-to-use strategy to constrain the conformation of a peptide with gold nanorods (AuNRs) for further use in near-infrared (NIR) photothermal therapy (Scheme 1). With terminal-thiol RGD (arginine, glycine, aspartic acid) sequence containing peptides, LA-RGDK-LA (LA: lipoic acid) and CRGDC (C: cysteine), the AuNRs act as structural constrainers *via* Au–S interactions to bend the flexible peptides and fix the RGD sequence to a rigid conformation. Besides the role of conformation constrainers, the AuNRs can also confer other advantageous features, such as properties for two-photon photoluminescence (TPPL) imaging and photothermal therapy, with respect to biomedical applications.[19–25]

AuNRs (48.5 × 15.5 nm) were prepared with a modified procedure from a previously reported seed-mediated growth method, and then modified with methoxy-PEG-thiol (mPEG-SH, MW = 1000 Da) to obtain AuNR-PEG. After reduction of the disulfides in the peptides LA-RGDK, *c*(CRGDC), and LA-RGDK-LA, AuNR-PEG was added into the reduced peptide solutions for conjugation of the peptides with AuNRs, and thus peptide-modified gold nanorods AuNR-LA-RGDK, AuNR-*c*(CRGDC) and AuNR-*c*(LA-RGDK-LA) were fabricated, respectively. Two sets of peptide-modified AuNRs were obtained, one set with the

[a]*School of Pharmaceutical Sciences, Capital Medical University, Beijing 100069, China. E-mail: cjfang@ccmu.edu.cn*

[b]*Beijing National Laboratory for Molecular Sciences, State Key Laboratory of Rare Earth Materials Chemistry and Applications, PKU-HKU Joint Laboratory in Rare Earth Materials and Bioinorganic Chemistry, College of Chemistry and Molecular Engineering, Peking University, Beijing 100871, China*

† Electronic supplementary information (ESI) available: Materials and methods, synthesis, and TPPL images and MFI data. See DOI: 10.1039/c8ra04379e

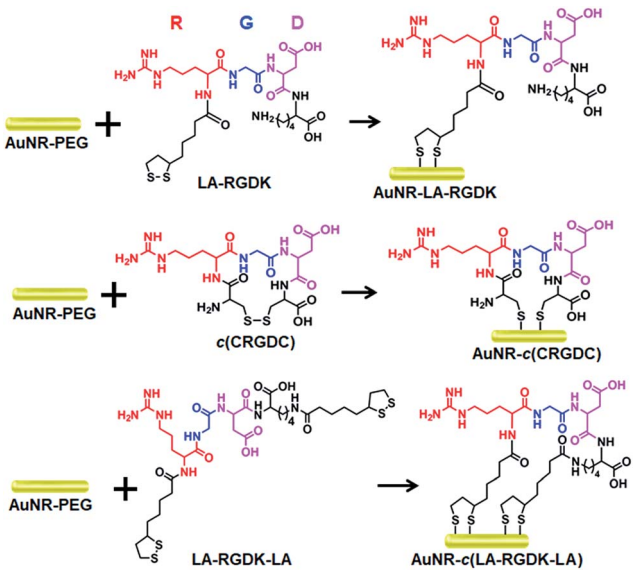

Scheme 1 Various peptide-modified AuNRs: AuNR-LA-RGDK, AuNR-*c*(CRGDC) and AuNR-*c*(LA-RGDK-LA).

number of peptides per AuNR as 5000 : 1 (Fig. 1A–C) and the other set with 20 000 protein molecules (Fig. 1D–F) per AuNR. The zeta-potentials of the various AuNRs modified with peptides of different kinds and numbers were measured and are listed in Table 1. The zeta-potentials changed from negative to positive as the ratio of the numbers of peptide molecules per nanoparticle increased from 5000 : 1 to 20 000 : 1. As shown in Fig. 2, the prepared AuNRs showed two typical local surface plasmon resonance (LSPR) bands, with transverse LSPR centred at 520 nm and longitude LSPR centred at 680 nm, respectively. After conjugation with various peptides, the LSPR bands of the two sets of AuNRs exhibited no significant changes.

Integrin is a critical mediator and regulator in physiological and pathological angiogenesis, including tumour angiogenesis. Therefore, this means that integrin is a very promising

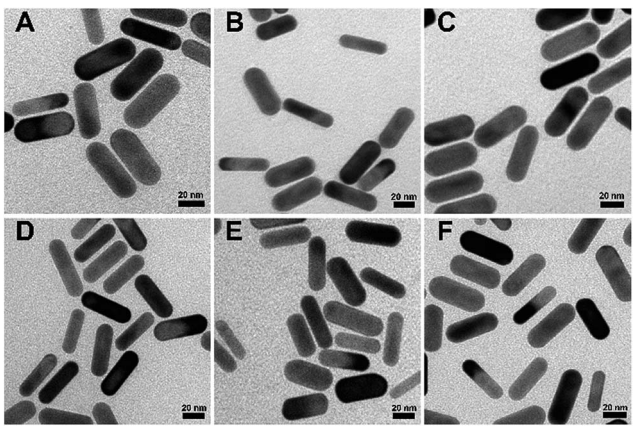

Fig. 1 Transmission electron microscope images of the two sets of AuNRs: AuNR-LA-RGDK, AuNR-*c*(CRGDC) and AuNR-*c*(LA-RGDK-LA), with ratios of peptides per AuNR of 5000 (A, B and C, respectively) and 20 000 (D, E, and F, respectively).

Table 1 Zeta-potentials of AuNRs modified with peptides of different kinds and numbers

Samples	Zeta-potential (5000 : 1) (mV)	Zeta-potential (20 000 : 1) (mV)
AuNR-LA-RGDK	−15.9 ± 0.5	13.8 ± 1.2
AuNR-*c*(CRGDC)	−13.8 ± 3.3	15.9 ± 1.6
AuNR-*c*(LA-RGDK-LA)	−19.5 ± 3.2	16.7 ± 1.0

therapeutic target and an excellent candidate for cancer therapy.[26–28] The recognition and mode of interaction between the integrin receptor and the RGD sequence is basic, and is the most predominant recognition motif involved in cell adhesion. Hence, the targeting efficiencies of AuNR-LA-RGDK, AuNR-*c*(CRGDC), and AuNR-*c*(LA-RGDK-LA) nanoparticles toward integrin were examined and compared through their cellular uptake by cancerous cells with different levels of integrin $\alpha_V\beta_3$ expression, A549 cells (high), HepG2 cells (medium) and MCF-7 cells (low) and doxorubicin resistant MCF-7/ADR cells (low) (the HepG2 cells were purchased from Keygen Biotec, and the MCF-7, MCF-7/ADR, and A549 cells were subcultured in our lab). Overall, the cellular uptake of the peptide-modified AuNRs was cell-line-dependent (Fig. 3 and 4) and correlated with $\alpha_V\beta_3$ levels, indicating that cellular uptake occurs through receptor-mediated endocytosis *via* integrin receptors on the membrane. As listed in Table 1, the values of the zeta-potentials are comparable for each set of AuNRs, therefore, the effect of surface potential of the various AuNRs on the cellular uptake of

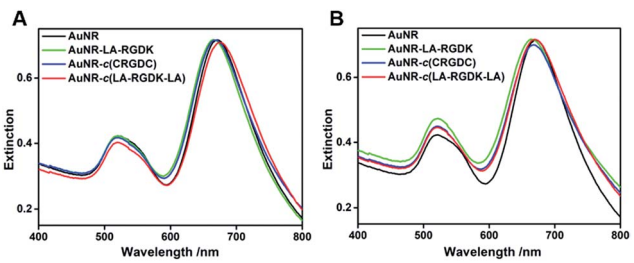

Fig. 2 The extinction spectra of the two sets of AuNR-LA-RGDK, AuNR-*c*(CRGDC) and AuNR-*c*(LA-RGDK-LA) in aqueous solution, with ratios of peptides per AuNR of 5000 : 1 (A) and 20 000 : 1 (B).

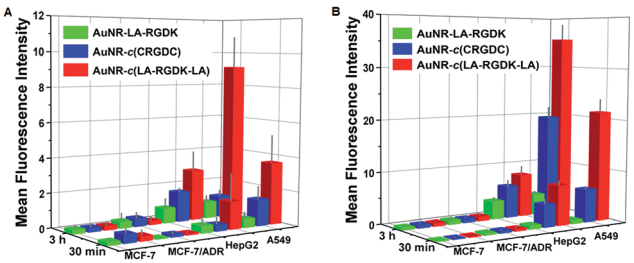

Fig. 3 The mean fluorescence intensities of MCF-7, MCF-7/ADR, HepG2, and A549 cells treated with AuNR-LA-RGDK, AuNR-*c*(CRGDC), and AuNR-*c*(LA-RGDK-LA) nanoparticles with ratios of 5000 : 1 (A) and 20 000 : 1 (B).

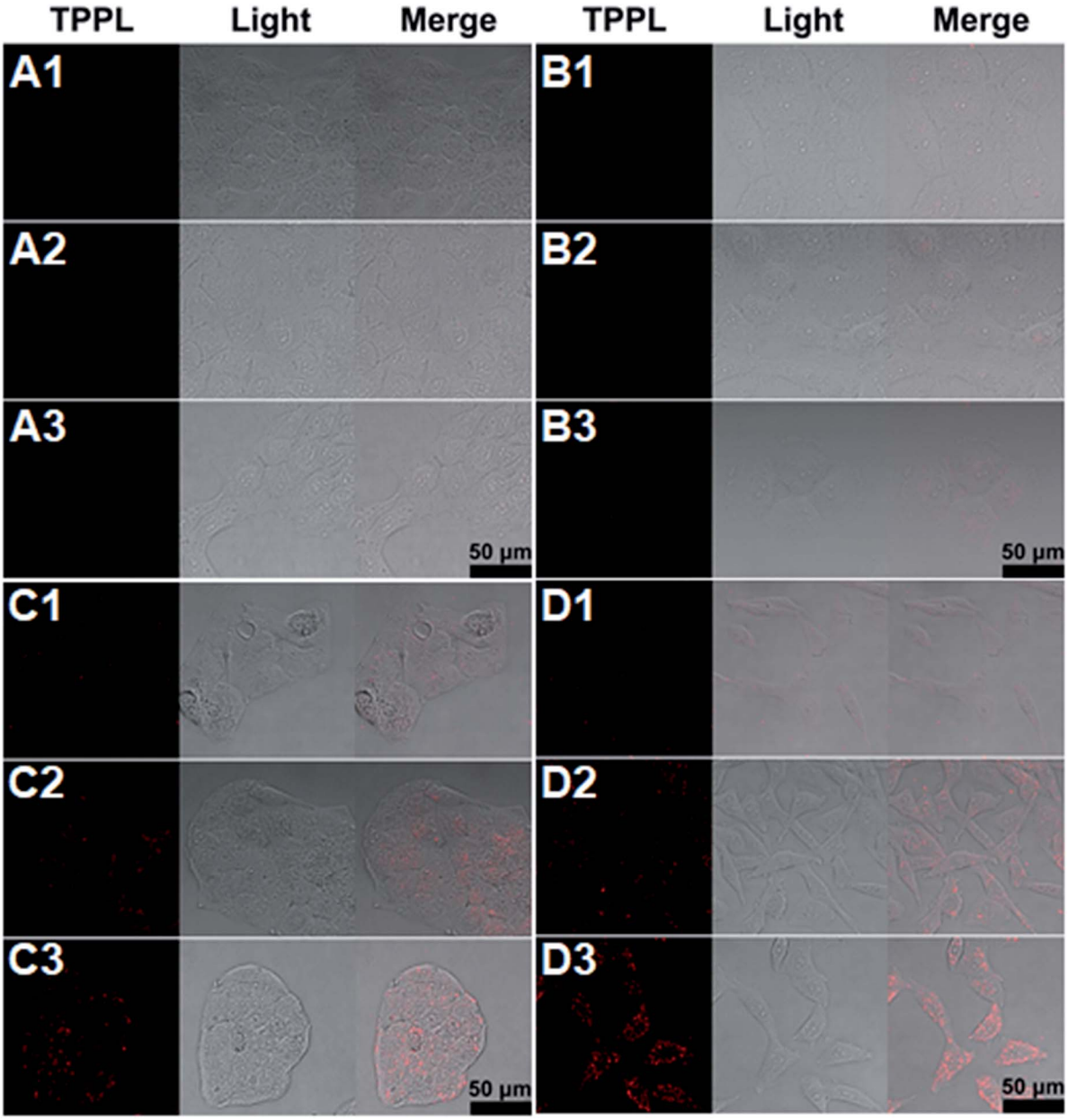

Fig. 4 TPPL images of intracellular AuNR-LA-RGDK (1), AuNR-*c*(CRGDC) (2), and AuNR-*c*(LA-RGDK-LA) (3) (ratio of peptides to AuNRs: 20 000 : 1) after incubation with MCF-7 (A), MCF-7/ADR (B), HepG2 (C), and A549 (D) cells for 30 min, respectively. The images were taken with an Olympus FVMPE-RS multiphoton laser scanning microscope under excitation at 730 nm with a 520–560 nm detector.

the nanoparticles could be rationally ignored, and integrin receptor-mediated endocytosis was thus the predominant way that the nanoparticles entered into the cells. For each cell line, the mean fluorescence intensity (MFI) of intracellular AuNR-*c*(LA-RGDK-LA) was the highest, and that of AuNR-LA-RGDK the lowest. In addition, no obvious difference between the MFI for MCF-7 and MCF-7/ADR was observed, suggesting that this strategy is powerless in overcoming multidrug resistance. This result confirms the existence of the receptor-mediated endocytosis cellular uptake pathway, and the rigid conformation of the RGD sequence is a predominant factor in integrin $\alpha_v\beta_3$-mediated endocytosis. With only one LA terminal of LA-RGDK fixed on the Au surface, the flexible conformation of the RGD sequence is retained, whereas for AuNR-*c*(LA-RGDK-LA), where two terminal LAs interact simultaneously with a single AuNR, the freedom of the RGD sequence is greatly restricted. Therefore, the conformation of LA-RGDK-LA is perturbed, and the restrictions imposed in the conjugation of the peptides with the AuNR surface makes the peptides adopt the specific rigid conformation that is required for the efficient binding to the RGD-sensitive receptor of integrin.

The cellular uptake of peptide-modified AuNRs is time-dependent. As the incubation time was prolonged from 0.5 h to 3 h, the MFI increased, implying increased cellular uptake

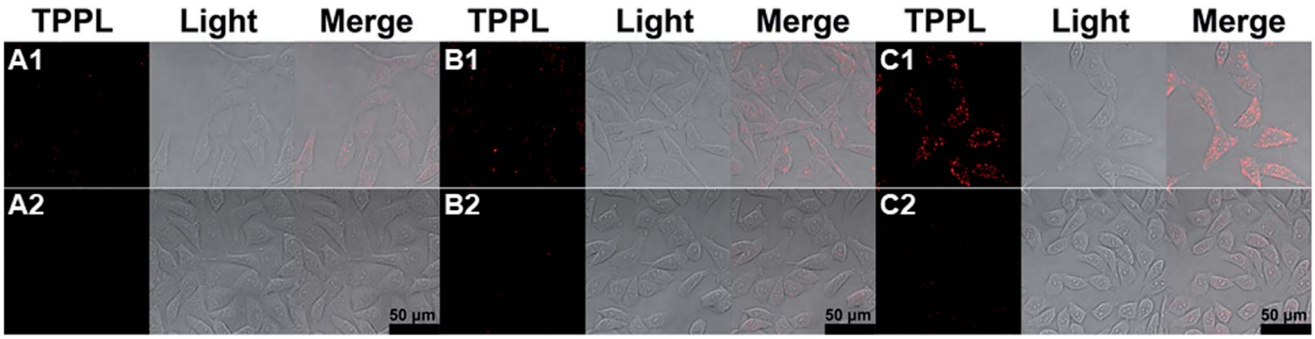

Fig. 5 Competition experiments with A549 cell incubated directly with AuNR-LA-RGDK (A), AuNR-*c*(CRGDC) (B), and AuNR-*c*(LA-RGDK-LA) (C) (1) (ratio of peptide to AuNR: 20 000 : 1), respectively, or pre-incubated with the efficient ligand *c*(RGDyK) and then incubated with the corresponding AuNRs (2).

(Fig. 4 and S1–S8 in the ESI†). The ratio of peptides per AuNR also played an important role. When the ratio of peptides per AuNR was increased from 5000 to 20 000 molecules per AuNR, the most profound differences for cellular uptake of AuNR-*c*(LA-RGDK-LA) and AuNR-LA-RGDK by A549 cell were amplified from 9.6- to 33.4-fold (Table S1 in ESI†). The cellular uptake results suggest that fixing the RGD sequence *via* interaction of LA with the AuNR surface is beneficial for bending the RGD sequence to a preferential rigid conformation for targeting the integrin receptor. This was further confirmed with the cellular uptake of RGDK, indicating the presence of the conformational constraint of the RGD sequence *via* interactions of the thiol groups of cysteine with the AuNRs surface. The targeting efficiency was different between AuNR-*c*(LA-RGDK-LA) and AuNR-*c*(CRGDC) groups, suggesting that other factors such as Au–S bond strength, peptide length, and variety of amino acids may also finely tune the conformation of the RGD sequence in the conjugation of the RGD-containing peptides with the AuNR surface, and therefore impose effects on the cellular uptake. With respect to this, it is necessary to further explore these effect and mechanisms in future work.

Further, the targeting efficiency of the RGD sequence was confirmed with a competition experiment by using A549 cells and the known ligand *c*(RGDyK) (Fig. 5 and Table S2†).[28] Without the effective integrin ligand *c*(RGDyK) to interact with the integrin receptor on the membrane, AuNR-LA-RGDK, AuNR-*c*(CRGDC), and AuNR-*c*(LA-RGDK-LA) could enter into the cells *via* receptor mediated endocytosis, and thus the TPPL of the AuNRs could be observed (Fig. 5A1–C1). In contrast, the intracellular TPPL was almost invisible when the receptor was blocked by the ligand *c*(RGDyK) after pre-incubation of the A549 cell with *c*(RGDyK) and thus the AuNR-LA-RGDK, AuNR-*c*(CRGDC), and AuNR-*c*(LA-RGDK-LA) could not be internalized by the cells.

To investigate hyperthermia effects, the temperature increase caused by the photothermal conversion of AuNR-*c*(LA-RGDK-LA) was recorded (Fig. 6). After irradiation with a laser at 808 nm, of the cells which were pre-incubated with AuNR-*c*(LA-RGDK-LA) for 3 h, the MCF-7 and HepG2 cell groups did not experience a significant temperature increase, with a ΔT of only up to 3 °C, due to the lower uptake of AuNR-*c*(LA-RGDK-LA). In contrast, the A549 group experienced a large degree of heat generation. This verifies the high uptake of AuNR-*c*(LA-RGDK-LA) and thereby the improved targeting ability toward the $\alpha_V\beta_3$ receptor. Thereafter, targeted photothermal treatment was

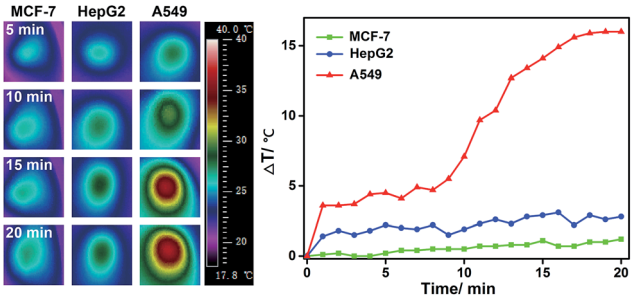

Fig. 6 IR images (left) and the corresponding temperature variation curves (right) after MCF-7, HepG2, and A549 cells were incubated with AuNR-*c*(LA-RGDK-LA) (ratio of peptides to AuNRs: 20 000 : 1) for 3 h, under irradiation at 808 nm with a power density of 2 W cm^{-2} as a function of irradiation time. The images were recorded with an infrared camera FOTRIC 225-3.

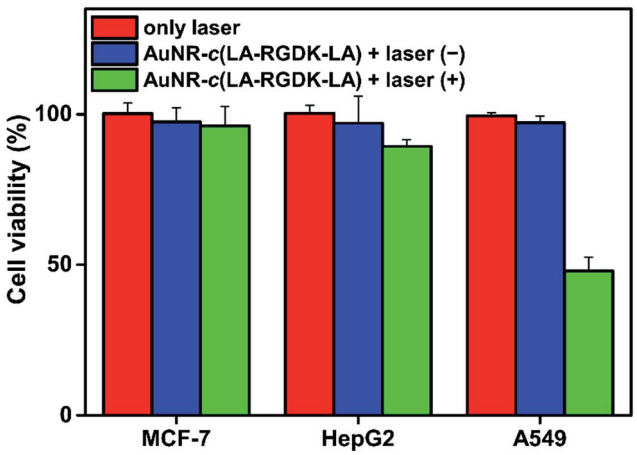

Fig. 7 Cell viability of MCF-7, HepG2 and A549 cells treated with AuNR-*c*(LA-RGDK-LA) (ratio of peptides to AuNRs: 20 000 : 1) with and without 808 nm laser irradiation at a power density of 2 W cm^{-2}.

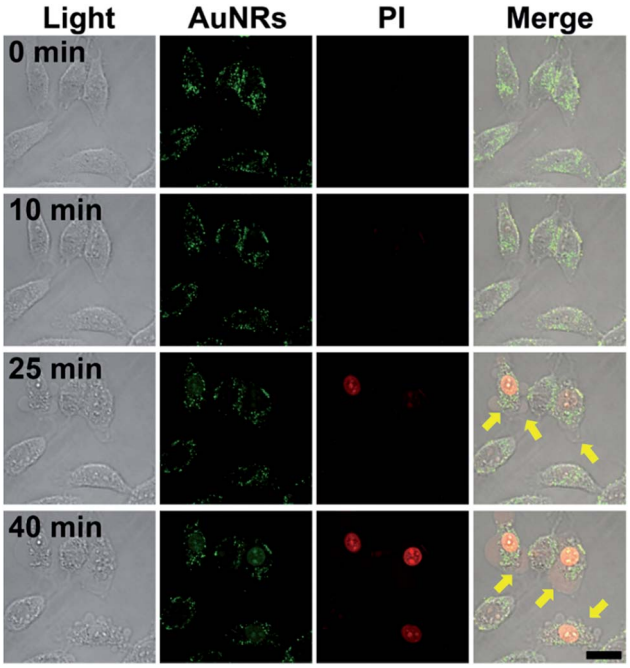

Fig. 8 TPPL images at various intervals after NIR photothermal therapy of A549 cells with AuNR-*c*(LA-RGDK-LA) (ratio of peptides to AuNRs: 20 000 : 1) irradiated by a laser at 730 nm. Green indicates the TPPL of the AuNRs. Cells were stained with propidium iodide (PI), and the red fluorescence indicated the nuclei of dead cells after laser irradiation. Yellow arrows indicate the microbubbles formed after irradiation. Scale bar: 10 μm.

further explored with MTT assays. The cells were pre-incubated with AuNR-*c*(LA-RGDK-LA) for 3 h and then treated with/without a laser. As shown in Fig. 7, the induced harm to the cells was insignificant without irradiation. If the laser was applied, the cell viability decreased remarkably, especially, for the A549 group, suggesting higher uptake by the A549 cell. The photothermal effects were further demonstrated with multiphoton laser scanning microscopy (Fig. 8). The A549 cells were first incubated with AuNR-*c*(LA-RGDK-LA) for 3 h and then stained with propidium iodide (PI), which only enters into dead cells. To visualize the microbubble-induced destruction of the cells within the irradiated regions, time-resolved images were recorded to monitor how the cell responded to the microbubbles formed right after laser irradiation (Fig. 8 and video in ESI†). After irradiation, a contraction of the cellular volume was observed as a result of localized mechanical destruction caused by the microbubbles that formed.[29,30] After about 25 min of irradiation, the intracellular PI fluorescence became stronger and stronger, but on the other hand, the cellular morphology gradually became irregular and the cells disintegrated to cellular debris.

Conclusions

In summary, we demonstrated a novel and easy-to-use strategy by anchoring RGD-containing peptides on AuNRs, and constraining the conformation to a preferential rigid one, to improve target ability. The strategy conveniently combines structural constraining of peptides with TPPL imaging and photothermal capabilities, which facilitates not only functional and intracellular characterization but also the biomedical application of potential peptide-based drugs, thus introducing a new tool for emerging demands in cancer therapy.

Conflicts of interest

There are no conflicts to declare.

Acknowledgements

The authors thank the NSFC (21571133, 21171120), the Beijing Natural Science Foundation Program and the Scientific Research Key Program of Beijing Municipal Commission of Education (KZ201710025024), and the Natural Science Foundation of Beijing Municipality (7132020). The authors also thank Zhongxin Xiao at the Core Facility Center, Capital Medical University for his kind support in multiphoton laser scanning microscopy.

Notes and references

1 R. Mercado-Lubo, Y. W. Zhang, L. Zhao, K. Rossi, X. Wu, Y. K. Zou, A. Castillo, J. Leonard, R. Bortell, D. L. Greiner, L. D. Shultz, G. Han and B. A. McCormick, *Nat. Commun.*, 2016, **7**, 12225.
2 B. Y. Lee, D. L. Clemens, A. Silva, B. J. Dillon, S. Masleša-Galić, S. Nava, X. T. Ding, C. M. Ho and M. A. Horwitz, *Nat. Commun.*, 2017, **10**, 1038.
3 D. Sobot, S. Mura and P. J. Couvreur, *J. Mater. Chem. B*, 2016, **4**, 5078–5100.
4 J. Vagner, H. C. Qu and V. Hruby, *Curr. Opin. Chem. Biol.*, 2008, **12**, 292–296.
5 J. E. Bock, J. Gavenonis and J. A. Krizer, *ACS Chem. Biol.*, 2013, **8**, 488–499.
6 R. Haubner, R. Gratias, B. Diefenbach, S. L. Goodman, A. Jonczyk and H. Kessler, *J. Am. Chem. Soc.*, 1996, **118**, 7461–7472.
7 E. Koivunen, B. Wang and E. Ruoslahti, *Nat. Biotechnol.*, 1995, **13**, 265–270.
8 R. Haubner, W. Schmitt, G. Hölzemann, S. L. Goodman, A. Jonczyk and H. Kessler, *J. Am. Chem. Soc.*, 1996, **118**, 7881–7891.
9 F. Danhier, A. L. Breton and V. Préat, *Mol. Pharm.*, 2012, **9**, 2961–2973.
10 M. A. Dechantsreiter, E. Planker, B. Mathä, E. Lohof, G. Hölzemann, A. Jonczyk, S. L. Goodman and H. Kessler, *J. Med. Chem.*, 1999, **42**, 3033–3040.
11 B. M. Lamb and M. N. Yousaf, *J. Am. Chem. Soc.*, 2011, **133**, 8870–8873.
12 J. Li, C. L. Sun, R. Shen, X. Y. Cao, B. Zhou, D. C. Bai and H. L. Zhang, *J. Am. Chem. Soc.*, 2014, **136**, 11050–11056.
13 M. T. Ma, H. N. Hoang, C. C. G. Scully, T. G. Appleton and D. P. Fair lie, *J. Am. Chem. Soc.*, 2009, **131**, 4505–4512.

14 Y. Liu, L. L. Li, G. B. Qi, X. G. Chen and H. Wang, *Biomaterials*, 2014, **35**, 3406–3415.
15 K. M. Mahar Doan, J. E. Humphreys, L. O. Webster, S. A. Wring, L. J. Shampine, C. J. Serabjit-Singh, K. K. Adkison and J. W. Polli, *J. Pharmacol. Exp. Ther.*, 2002, **303**, 1029–1037.
16 E. Y. Zhang, M. A. Phelps, C. Cheng, S. Ekins and P. W. Swaan, *Adv. Drug Delivery Rev.*, 2002, **54**, 329–354.
17 X. C. Ma, J. L. Jia, R. Cao, X. B. Wang and H. Fei, *J. Am. Chem. Soc.*, 2014, **136**, 17734–17737.
18 C. Kim, E. C. Cho, J. Y. Chen, K. H. Song, L. Au, C. Favazza, Q. Zhang, C. M. Cobley, F. Gao, Y. N. Xia and L. V. Wang, *ACS Nano*, 2010, **4**, 4559–4564.
19 M. F. Rosenberg, A. B. Kamis, R. Callaghan, C. F. Higgins and R. C. Ford, *J. Biol. Chem.*, 2003, **278**, 8294–8299; M. F. Rosenberg, R. Callaghan, S. Modok, C. F. Higgins and R. C. Ford, *J. Biol. Chem.*, 2005, **280**, 2857–2862.
20 K. König, *J. Microsc.*, 2000, **200**, 83–104.
21 A. A. Bhirde, B. V. Chikkaveeraiah, A. Srivatsan, G. Niu, A. J. Jin, A. Kapoor, Z. Wang, S. Patel, V. Patel, A. M. Gorbach, R. D. Leapman, J. S. Gutkind, A. R. Hight Walker and X. Y. Chen, *ACS Nano*, 2014, **8**, 4177–4189.
22 D. Jaque, L. Martínez Maestro, B. del Rosal, P. Haro-Gonzalez, A. Benayas, J. L. Plaza, E. M. Rodrígueza and J. G. Solé, *Nanoscale*, 2014, **6**, 9494–9530.
23 J. H. Liu, Y. X. Zhao, Q. Q. Guo, Z. Wang, H. Y. Wang, Y. X. Yang and Y. Z. Huang, *Biomaterials*, 2012, **33**, 6155–6161.
24 J. R. Starkey, A. K. Rebane, M. A. Drobizhev, F. Q. Meng, A. J. Gong, A. Elliott, K. Mclnnerney and C. W. Spangler, *Clin. Cancer Res.*, 2008, **14**, 6564–6573.
25 J. B. Song, X. Y. Yang, O. Jacobson, L. Lin, P. Huang, G. Niu, Q. J. Ma and X. Y. Chen, *ACS Nano*, 2015, **9**, 9199–9209.
26 C. Mas-Moruno, F. Rechenmacher and H. Kessler, *Anti-Cancer Agents Med. Chem.*, 2010, **10**, 753–768.
27 D. A. Reardon, K. L. Fink, T. Mikkelsen, T. F. Cloughesy, A. O'Neill, S. Plotkin, M. Glantz, P. Ravin, J. J. Raizer, K. M. Rich, D. Schiff, W. R. Shapiro, S. Burdette-Radoux, E. J. Dropcho, S. M. Wittemer, J. Nippgen, M. Picard and L. B. Nabors, *J. Clin. Oncol.*, 2008, **26**, 5610–5617.
28 J. Xie, K. Chen, H. Y. Lee, C. J. Xu, A. R. Hsu, S. Peng, X. Y. Chen and S. H. Sun, *J. Am. Chem. Soc.*, 2008, **130**, 7542–7543.
29 S. T. Wang, K. J. Chen, T. H. Wu, H. Wang, W. Y. Lin, M. Ohash, P. Y. Chiou and H. R. Tseng, *Angew. Chem., Int. Ed. Engl.*, 2010, **49**, 3777–3781.
30 E. Y. Hleb, Y. Hu, R. A. Drezek, J. H. Hafner and D. O. Lapotko, *Nanomedicine*, 2008, **3**, 797–812.